

A Randomized Algorithm for Tensor Singular Value Decomposition Using an Arbitrary Number of Passes

Salman Ahmadi-Asl[†]

Abstract—Computation of a tensor singular value decomposition (t-SVD) with a few number of passes over the underlying data tensor is crucial in using modern computer architectures, where the main concern is the communication cost. The current subspace randomized algorithms for computation of the t-SVD, need $2q + 2$ number of passes over the data tensor where q is an non-negative integer number (power iteration parameter). In this paper, we propose a new and flexible randomized algorithm which works for any number of passes v , not necessarily being an even number. It is a generalization of the methods developed for matrices to tensors. The expected error bound of the proposed algorithm is derived. Several numerical experiments are conducted and the results confirmed that the proposed algorithm is efficient and applicable. We also use our proposed method to develop a fast algorithm for tensor completion problem.

Index Terms—Tubal tensor decomposition, randomization, fixed-precision algorithm.

Multidimensional arrays or tensors are natural extensions of matrices and vectors. It was in 1927 when the first definition of the tensor rank was presented and the corresponding tensor decomposition termed Canonical Polyadic Decomposition (CPD) was defined [1]. Later on, an alternative definition for the tensor rank (Tucker rank) was defined in [2], [3] and a new tensor decomposition called Tucker decomposition was proposed. The Tucker decomposition includes the CPD as a special case. It turned out that there is no a unique definition for the tensor rank and the tensor decomposition. Other tensor decompositions include Tensor Train (TT) or Matrix Product State (MPS) [4], [5], Tensor Chain/Ring (TC) or MPS with periodic boundary conditions [6], [7], tensor SVD (t-SVD) [8], [9] and Hierarchical Tucker decomposition [10]. Tensors have been successfully applied in many machine learning and data analysis tasks such as data reconstruction, data compression, clustering, etc. see [11], [12] and the references therein for a comprehensive review on such applications. One of the main challenges in this topic is developing fast algorithms for computation of the tensors decompositions. For example, for solving the tensor completion problem [13], we usually need to compute tensor decompositions multiple times. These computations are prohibitive when the data tensors are large-scale or many iterations are required for the convergence. Hence, we need to develop fast algorithms for tensor decompositions to be used in real applications. The randomization has been proved to be an efficient framework for low-rank matrix computation [14] and recently was generalized to the

tensors [15], [16], [17]. Randomized algorithms reduce the computational complexity of the deterministic counterparts and also their communication cost. The latter benefit is especially important when the data tensor is very large and stored in several machines. Here, the communication cost is the main concern and we need to access the data tensor as few as possible. In the context of randomization, such methods are called randomized pass-efficient algorithms [18]. The standard randomized subspace iteration, needs $2q + 2$ passes/views (q is a power iteration parameter) over the data tensor [14]. In [18], the author proposed new randomized algorithms which do not have this limitation and for any budget of passes, it can compute a low-rank matrix approximation. In this paper, we generalize this idea to the tensor case based on the tubal product (t-product) [8], [9]. Simulations on the synthetic and real-world datasets are provided to support the theoretical results. In particular, we present an application of the proposed algorithm to the image/video completion problem.

Our principal contributions can be summarized as follows:

- Developing a pass-efficient randomized algorithm for computation of the t-SVD with an arbitrary number of passes
- Applying the proposed algorithm to the image/video completion problem
- Extensive simulation results on synthetic and real-world datasets

The remainder of this paper is organized as follows: The preliminary concepts and definitions are introduced in Section I. Section II is devoted to introducing the t-SVD and its computational procedures. The proposed approaches are outlined in Section III. Simulation results are presented in Section V and a conclusion is given in Section VI.

I. PRELIMINARIES

Let us introduce the notations and main concepts that we need in the next sections. Tensors, matrices and vectors are denoted by underlined bold upper case letters e.g., $\underline{\mathbf{X}}$, bold upper case letters, e.g., \mathbf{X} and bold lower case letters, e.g., \mathbf{x} , respectively. Slices are produced by fixing two modes of a tensor. For a 3rd order tensor $\underline{\mathbf{X}}$, $\mathbf{X}(:, :, i)$, $\mathbf{X}(:, i, :)$ and $\mathbf{X}(i, :, :)$ are called frontal, lateral and horizontal slices. Fibers are produced by fixing one mode, for a 3rd order tensor $\underline{\mathbf{X}}$, $\mathbf{X}(i, j, :)$ is called a tube. The Frobenius and infinity norms

[†]Skolkovo Institute of Science and Technology (SKOLTECH), Center for Artificial Intelligence Technology, Moscow, Russia, E-mail: s.asl@skoltech.ru.

of tensors are denoted by $\|\cdot\|_F$ and $\|\cdot\|_\infty$, respectively. The notation ‘‘conj’’ denotes the complex conjugate of a complex number or the component-wise complex conjugate of a matrix. The mathematical expectation of a random tensor $\underline{\mathbf{X}}$ is denoted by $\mathbb{E}(\underline{\mathbf{X}})$ and $\lceil n \rceil$ means the nearest integer number greater than or equal to n . For a given data tensor $\underline{\mathbf{X}} \in \mathbb{R}^{I_1 \times I_2 \times \dots \times I_N}$ and the observation index set $\underline{\Omega} \in \mathbb{R}^{I_1 \times I_2 \times \dots \times I_N}$, the projector $\mathbf{P}_{\underline{\Omega}}$ is defined as follows

$$\mathbf{P}_{\underline{\Omega}}(\underline{\mathbf{X}}) = \begin{cases} \underline{\mathbf{X}}(\mathbf{i}) & \mathbf{i} \in \underline{\Omega}, \\ 0 & \mathbf{i} \notin \underline{\Omega}, \end{cases}$$

where $\mathbf{i} = (i_1, i_2, \dots, i_N)$ is an arbitrary multi-index with $1 \leq i_n \leq I_n$, $n = 1, 2, \dots, N$. Throughout the paper, we focus only on real and 3rd order tensors, however, our results can be generalized to complex higher order tensor tensors straightforwardly.

In order to introduce the t-SVD, we first need to present some basic definitions such as the t-product operation and f-diagonal tensors.

Definition 1. (t-product) Let $\underline{\mathbf{X}} \in \mathbb{R}^{I_1 \times I_2 \times I_3}$ and $\underline{\mathbf{Y}} \in \mathbb{R}^{I_2 \times I_4 \times I_3}$, then the t-product $\underline{\mathbf{X}} * \underline{\mathbf{Y}} \in \mathbb{R}^{I_1 \times I_4 \times I_3}$ is defined as follows

$$\underline{\mathbf{C}} = \underline{\mathbf{X}} * \underline{\mathbf{Y}} = \text{fold}(\text{circ}(\underline{\mathbf{X}}) \text{unfold}(\underline{\mathbf{Y}})), \quad (1)$$

where

$$\text{circ}(\underline{\mathbf{X}}) = \begin{bmatrix} \underline{\mathbf{X}}(:, :, 1) & \underline{\mathbf{X}}(:, :, I_3) & \dots & \underline{\mathbf{X}}(:, :, 2) \\ \underline{\mathbf{X}}(:, :, 2) & \underline{\mathbf{X}}(:, :, 1) & \dots & \underline{\mathbf{X}}(:, :, 3) \\ \vdots & \vdots & \ddots & \vdots \\ \underline{\mathbf{X}}(:, :, I_3) & \underline{\mathbf{X}}(:, :, I_3 - 1) & \dots & \underline{\mathbf{X}}(:, :, 1) \end{bmatrix},$$

and

$$\text{unfold}(\underline{\mathbf{Y}}) = \begin{bmatrix} \underline{\mathbf{Y}}(:, :, 1) \\ \underline{\mathbf{Y}}(:, :, 2) \\ \vdots \\ \underline{\mathbf{Y}}(:, :, I_3) \end{bmatrix}, \quad \underline{\mathbf{Y}} = \text{fold}(\text{unfold}(\underline{\mathbf{Y}})).$$

It is known that the t-product operation indeed is the circular convolution operator and can be computed using Fast Fourier Transform (FFT). To this end, the FFT is applied to all tubes of two tensors $\underline{\mathbf{X}}$, $\underline{\mathbf{Y}}$, and obtain new tensors $\widehat{\underline{\mathbf{X}}}$, $\widehat{\underline{\mathbf{Y}}}$. Then, we multiply the frontal slices of the tensors $\widehat{\underline{\mathbf{X}}}$, $\widehat{\underline{\mathbf{Y}}}$ to get the new tensor $\widehat{\underline{\mathbf{Z}}}$. Finally, we apply the Inverse FFT (IFFT) to all tubes of the tensor $\widehat{\underline{\mathbf{Z}}}$. This procedure is summarized in Algorithm 1. This is the optimized version of the t-product which needs only the FFT of the first $\lceil \frac{I_3+1}{2} \rceil$ frontal slices suggested by Lu et al. in [19] while the original paper ([8], [9]) consider the FFT of all frontal slices. Note that $\text{fft}(\underline{\mathbf{Z}}, [], 3)$ is equivalent to computing the FFT of all tubes of the tensor $\underline{\mathbf{Z}}$. The t-product can be defined according to an arbitrary invertible transform [20]. For example, the unitary transform matrices are utilized in [21], instead of discrete Fourier transform matrices. It was also proposed in [22] to use non-invertible transforms instead of unitary matrices.

It can be proved that for a tensor $\underline{\mathbf{X}} \in \mathbb{R}^{I_1 \times I_2 \times I_3}$, we have

$$\|\underline{\mathbf{X}}\|_F^2 = \frac{1}{I_3} \sum_{i=1}^{I_3} \widehat{\underline{\mathbf{X}}}(:, :, i), \quad (2)$$

where $\widehat{\underline{\mathbf{X}}}(:, :, i)$ is the i -th frontal slice of the tensor $\widehat{\underline{\mathbf{X}}} = \text{fft}(\underline{\mathbf{X}}, [], 3)$, see [23].

Algorithm 1: t-product in the Fourier domain [8]

Input : Two data tensors
 $\underline{\mathbf{Z}} \in \mathbb{R}^{I_1 \times I_2 \times I_3}$, $\underline{\mathbf{X}} \in \mathbb{R}^{I_2 \times I_4 \times I_3}$
Output: t-product $\underline{\mathbf{C}} = \underline{\mathbf{Z}} * \underline{\mathbf{X}} \in \mathbb{R}^{I_1 \times I_4 \times I_3}$
1 $\widehat{\underline{\mathbf{Z}}} = \text{fft}(\underline{\mathbf{Z}}, [], 3)$
2 $\widehat{\underline{\mathbf{X}}} = \text{fft}(\underline{\mathbf{X}}, [], 3)$
3 **for** $i = 1, 2, \dots, \lceil \frac{I_3+1}{2} \rceil$ **do**
4 | $\widehat{\underline{\mathbf{C}}}(:, :, i) = \widehat{\underline{\mathbf{Z}}}(:, :, i) \widehat{\underline{\mathbf{X}}}(:, :, i)$
5 **end**
6 **for** $i = \lceil \frac{I_3+1}{2} \rceil + 1, \dots, I_3$ **do**
7 | $\widehat{\underline{\mathbf{C}}}(:, :, i) = \text{conj}(\widehat{\underline{\mathbf{C}}}(:, :, I_3 - i + 2))$
8 **end**
9 ; $\underline{\mathbf{C}} = \text{ifft}(\widehat{\underline{\mathbf{C}}}, [], 3)$

Definition 2. (Transpose) Let $\underline{\mathbf{X}} \in \mathbb{R}^{I_1 \times I_2 \times I_3}$ be a given tensor. Then the complex conjugate transpose of tensor $\underline{\mathbf{X}}$ is denoted by $\underline{\mathbf{X}}^T \in \mathbb{R}^{I_2 \times I_1 \times I_3}$ which is constructed by applying transpose to all its frontal slices and reversing the order of second till last transposed frontal slices.

Definition 3. (Identity tensor) Identity tensor $\underline{\mathbf{I}} \in \mathbb{R}^{I_1 \times I_1 \times I_3}$ is a tensor whose first frontal slice is an identity matrix of size $I_1 \times I_1$ and all other frontal slices are zero. It is easy to show $\underline{\mathbf{I}} * \underline{\mathbf{X}} = \underline{\mathbf{X}}$ and $\underline{\mathbf{X}} * \underline{\mathbf{I}} = \underline{\mathbf{X}}$ for all tensors of conforming sizes.

Definition 4. (Orthogonal tensor) A tensor $\underline{\mathbf{X}} \in \mathbb{R}^{I_1 \times I_1 \times I_3}$ is orthogonal (under t-product operator) if $\underline{\mathbf{X}}^T * \underline{\mathbf{X}} = \underline{\mathbf{X}} * \underline{\mathbf{X}}^T = \underline{\mathbf{I}}$.

Definition 5. (f-diagonal tensor) If all frontal slices of a tensor are diagonal then the tensor is called f-diagonal.

Definition 6. (Random tensor) A tensor $\underline{\Omega}$ is random if its first frontal slice $\underline{\mathbf{X}}(:, :, 1)$ has independent and identically distributed (i.i.d) elements while the other frontal slices are zero.

The MATLAB implementation of many operations in t-product format can be found in the useful toolbox <https://github.com/canyilu/Tensor-tensor-product-toolbox>.

II. TUBAL SVD AND TUBAL QR DECOMPOSITION

Tubal SVD (t-SVD) was originally proposed in ([8], [9], [24], [25]) to represent a 3rd-order tensor as a product of three 3rd-order tensors where all frontal slices of the middle tensor are diagonal, (Figure 1, provides a graphical illustration on the t-SVD and its truncated version). For generalization of the t-SVD to higher order tensors see [26].

The tubal rank is defined as the number of nonzero tubes of the middle tensor. It is interesting that unlike other tensor decompositions, the truncated t-SVD provides the best approximation in the least-squares sense for any unitary invariant tensor norm [8].

Let $\underline{\mathbf{X}} \in \mathbb{R}^{I_1 \times I_2 \times I_3}$, then the t-SVD of the tensor $\underline{\mathbf{X}}$, admits the model $\underline{\mathbf{X}} = \underline{\mathbf{U}} * \underline{\mathbf{S}} * \underline{\mathbf{V}}^T$, where $\underline{\mathbf{U}} \in \mathbb{R}^{I_1 \times R \times I_3}$, $\underline{\mathbf{V}} \in \mathbb{R}^{R \times I_2 \times I_3}$ are orthogonal tensors and the tensor $\underline{\mathbf{S}} \in \mathbb{R}^{R \times R \times I_3}$

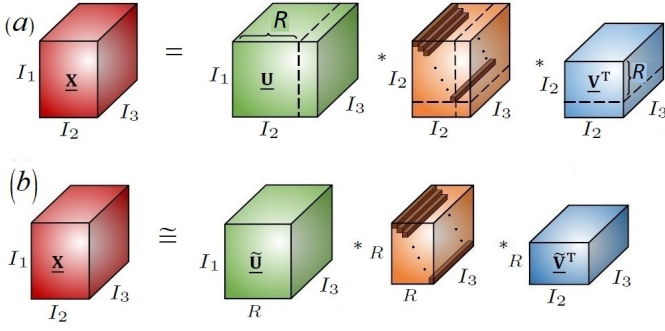


Fig. 1. Illustration of (a) Tubal SVD (t-SVD) and (b) truncated t-SVD for a 3rd-order tensor [27].

is f -diagonal ([8], [9]). Computation of the t-SVD is performed in the Fourier domain and this is summarized in Algorithm 2. Similar to the t-product, this Algorithm 2 is a faster version of the original truncated t-SVD developed by Lu et al. in [19] which the SVD of the only first slices are required [19]. The original t-SVD [8], [9] involves the SVD of all frontal slices in the Fourier domain. Similar to the t-product, instead of the discrete Fourier transform matrices, one can define the t-SVD according to an arbitrary unitary transform matrix. It is shown in [22] that this can provide t-SVD with a lower tubal rank.

Algorithm 2: Truncated t-SVD

Input : A data tensor $\underline{\mathbf{X}} \in \mathbb{R}^{I_1 \times I_2 \times I_3}$ and a target tubal rank R ;
Output: $\underline{\mathbf{U}}_R \in \mathbb{R}^{I_1 \times R \times I_3}$, $\underline{\mathbf{S}}_R \in \mathbb{R}^{R \times R \times I_3}$, $\underline{\mathbf{V}}_R \in \mathbb{R}^{I_2 \times R \times I_3}$;

- 1 $\widehat{\underline{\mathbf{X}}} = \text{fft}(\underline{\mathbf{X}}, [], 3)$;
- 2 **for** $i = 1, 2, \dots, \lceil \frac{I_3+1}{2} \rceil$ **do**
- 3 $[\underline{\mathbf{U}}, \underline{\mathbf{S}}, \underline{\mathbf{V}}] = \text{TruncatedSVD}(\widehat{\underline{\mathbf{X}}}(:, :, i), R)$;
- 4 $\widehat{\underline{\mathbf{U}}}(:, :, i) = \underline{\mathbf{U}}$;
- 5 $\widehat{\underline{\mathbf{S}}}(:, :, i) = \underline{\mathbf{S}}$;
- 6 $\widehat{\underline{\mathbf{V}}}(:, :, i) = \underline{\mathbf{V}}$;
- 7 **end**
- 8 **for** $i = \lceil \frac{I_3+1}{2} \rceil + 1, \dots, I_3$ **do**
- 9 $\widehat{\underline{\mathbf{U}}}(:, :, i) = \widehat{\underline{\mathbf{U}}}(:, :, I_3 - i + 2)$;
- 10 $\widehat{\underline{\mathbf{S}}}(:, :, i) = \widehat{\underline{\mathbf{S}}}(:, :, I_3 - i + 2)$;
- 11 $\widehat{\underline{\mathbf{V}}}(:, :, i) = \widehat{\underline{\mathbf{V}}}(:, :, I_3 - i + 2)$
- 12 **end**
- 13 ; $\underline{\mathbf{U}}_R = \text{ifft}(\widehat{\underline{\mathbf{U}}}, [], 3)$, $\underline{\mathbf{S}}_R = \text{ifft}(\widehat{\underline{\mathbf{S}}}, [], 3)$,
- 14 $\underline{\mathbf{V}}_R = \text{ifft}(\widehat{\underline{\mathbf{V}}}, [], 3)$.

The tubal QR computation can be defined similarly based on the t-product. To be precise, for the tubal QR decomposition of a tensor $\underline{\mathbf{X}} \in \mathbb{R}^{I_1 \times I_2 \times I_3}$, i.e., $\underline{\mathbf{X}} = \underline{\mathbf{Q}} * \underline{\mathbf{R}}$, we first compute the FFT of the tensor $\underline{\mathbf{X}}$ as

$$\widehat{\underline{\mathbf{X}}} = \text{fft}(\underline{\mathbf{X}}, [], 3), \quad (3)$$

and then the QR decompositions of all frontal slices of the

tensor $\widehat{\underline{\mathbf{X}}}$ are computed as follows

$$\widehat{\underline{\mathbf{X}}}(:, :, i) = \widehat{\underline{\mathbf{Q}}}(:, :, i) \widehat{\underline{\mathbf{R}}}(:, :, i). \quad (4)$$

Finally the IFFT operator is applied to the tensors $\widehat{\underline{\mathbf{Q}}}$ and $\widehat{\underline{\mathbf{R}}}$, to compute the tensors $\underline{\mathbf{Q}}$ and $\underline{\mathbf{R}}$. A given data tensor $\underline{\mathbf{X}}$, can be orthogonalized by applying the t-QR decomposition and taking the $\underline{\mathbf{Q}}$ part. We use the notation $\text{orth}(\underline{\mathbf{X}})$ to denote this operation. It is not difficult to see that the t-SVD and the t-QR decomposition for matrices ($I_3 = 1$) are reduced to the classical matrix SVD and QR decomposition. Here, $\text{orth}(\underline{\mathbf{X}})$ gives the orthogonal part of the matrix QR decomposition. In Matlab, this is equivalent to $\underline{\mathbf{Q}} = \text{qr}(\underline{\mathbf{X}}, 0)$. The tubal LU (t-LU) decomposition can be defined in an analogous way by replacing LU decomposition with the QR decomposition in (4).

III. A PASS EFFICIENT RANDOMIZED ALGORITHM FOR COMPUTATION OF THE T-SVD

It is obvious that Algorithm 2 is prohibitive for large-scale tensors because of multiple SVDs computations of some large-scale matrices. Let us describe the idea of random projection technique [23], [28], [29] to tackle this problem. In the first stage of the random projection method, the size of a given data tensor $\underline{\mathbf{X}}$ is reduced by multiplying the tensor $\underline{\mathbf{X}}$ with a random tensor as $\underline{\mathbf{Y}} = \underline{\mathbf{X}} * \underline{\Omega}$ where $\underline{\Omega} \in \mathbb{R}^{I_2 \times (R+P) \times I_3}$ is a random tensor. Then, the tensor $\underline{\mathbf{X}}$ is orthogonalized through the t-QR decomposition of the tensor $\underline{\mathbf{Y}}$ as follows

$$\underline{\mathbf{X}} \cong \underline{\mathbf{Q}} * \underline{\mathbf{B}}, \quad (5)$$

where $\underline{\mathbf{B}} = \underline{\mathbf{Q}}^T * \underline{\mathbf{X}}$, and $\underline{\mathbf{Q}} \in \mathbb{R}^{I_1 \times R \times I_3}$, $\underline{\mathbf{B}} \in \mathbb{R}^{R \times I_2 \times I_3}$. Note $R + P \ll I_2$, where \bar{R} is an estimation of the tubal-rank and P is the *oversampling* parameter for better capturing the action of the tensor $\underline{\mathbf{X}}$ [23]. From low tubal-rank approximation (5), and the t-SVD of $\underline{\mathbf{B}}$ as $\underline{\mathbf{B}} = \underline{\hat{\mathbf{U}}} * \underline{\hat{\mathbf{S}}} * \underline{\hat{\mathbf{V}}}^T$, we can recover the t-SVD of $\underline{\mathbf{X}}$ as $\underline{\mathbf{X}} = (\underline{\hat{\mathbf{Q}}} * \underline{\hat{\mathbf{U}}}) * \underline{\hat{\mathbf{S}}} * \underline{\hat{\mathbf{V}}}^T$. It is worth to mention that the tensor $\underline{\mathbf{B}}$ is smaller than the original data tensor $\underline{\mathbf{X}}$ and requires less memory and computational resources. This approach is efficient when the singular values of the frontal slices decay very fast otherwise the power iteration should be utilized. Here, the original tensor $\underline{\mathbf{X}}$ is replaced with $\underline{\mathbf{Z}} = (\underline{\mathbf{X}} * \underline{\mathbf{X}}^T)^q * \underline{\mathbf{X}}$ and the above-mentioned procedure is applied to $\underline{\mathbf{Z}}$. Due to stability issues, the tensor $\underline{\mathbf{Z}}$ should not be explicitly computed. Instead, it can be efficiently computed using the subspace iteration method [14], [23].

The basic randomized algorithm for the low-rank matrix approximation is summarized in Algorithm 3. The "for" loop (Lines 3-6), is the power iteration technique and is used when the singular values of a matrix do not decay fast. It has been confirmed that in practice $q = 1, 2, 3$ are sufficient to achieve good accuracy. Besides, P is the oversampling parameter which helps to better capture the range of the matrix. These strategies have been generalized to develop fast algorithms for computation of the tensor SVD (t-SVD). Algorithm 5, an extension of Algorithm 5 to the case of tensors, based on the t-product. For computational efficiency, one can replace the t-QR decomposition in Algorithm 5 and

6 with the t-LU decomposition [30], [31], or alternatively use a combination of t-QR and t-LU decompositions [30], [32]. Similar to Algorithm 3, the power iteration procedure discussed earlier is performed in Algorithm 6, in Lines (3-6). For power iteration q , Algorithm 5 needs to pass the data tensor $2q + 2$ times. Indeed, two passes for lines (2-7) and $2q$ passes for lines (3-6) of Algorithm 5. This means that the number of passes over the data tensor is always an even number. To the best of our knowledge, the only paper which proposes a single-pass randomized algorithm for computation of the t-SVD is [28] which is the generalization of those proposed in [33] from matrices to tensors. In [18], the authors resolved this drawback for matrices and developed randomized algorithms which are applicable for a budget of any number of passes. Motivated by these efficient algorithms, we extended them to the tensor case based on the t-product. Also in [34] a pass-efficient randomized algorithm is developed for the Tucker decomposition. In this paper we focus on the t-SVD and develop an efficient randomized algorithm which for any budget of passes, it can compute a low tubal rank approximation of the underlying data tensor. Besides, we exploit the proposed method to develop a fast algorithm to solve the tensor completion problem.

Now, we describe the main procedure for computation of the t-SVD in a pass-efficient way. Assume that we afford a budget v passes (the number of possible passes) for computation of the t-SVD, it is clear that if $v \geq 4$ is even, then we can use the classical randomized subspace Algorithm 3 with power iteration parameter $q = (v - 2)/2$. So, the question is how about having an odd number of passes?

Inspired by the idea presented in [18], we suggest the following procedures for computation of the t-SVD given $v \geq 2$ number of passes:

- (If v is even) Constructing an orthonormal tensor $\underline{\mathbf{Q}}$ for the range of the tensor $(\underline{\mathbf{X}} * \underline{\mathbf{X}}^T)^{(v-2)/2} * \underline{\mathbf{X}} * \underline{\mathbf{\Omega}}$. Then compute the truncated t-SVD of the tensor $(\underline{\mathbf{X}}^T * \underline{\mathbf{Q}})$ as

$$[\underline{\mathbf{V}}, \underline{\mathbf{S}}, \underline{\widehat{\mathbf{U}}}] = \text{Truncated t-SVD}(\underline{\mathbf{X}}^T * \underline{\mathbf{Q}})$$

and set $\underline{\mathbf{U}} = \underline{\mathbf{Q}} * \underline{\widehat{\mathbf{U}}}$.

- (If v is odd) Constructing an orthonormal tensor $\underline{\mathbf{Q}}$ for the range of the tensor $(\underline{\mathbf{X}}^T * \underline{\mathbf{X}})^{(v-1)/2} * \underline{\mathbf{\Omega}}$. Then compute the truncated t-SVD of the tensor as

$$[\underline{\mathbf{U}}, \underline{\mathbf{S}}, \underline{\widehat{\mathbf{V}}}] = \text{Truncated t-SVD}(\underline{\mathbf{X}}^T * \underline{\mathbf{Q}})$$

and set $\underline{\mathbf{V}} = \underline{\mathbf{Q}} * \underline{\widehat{\mathbf{V}}}$.

The next theorem gives the upper bound of the approximated tensor computed by Algorithm 3 and we use it to derive similar results for Algorithm 4.

Theorem 1. [23] (Average Frobenius error for Algorithm 3). Let $\mathbf{X} \in \mathbb{R}^{I_1 \times I_2}$ and $\mathbf{\Omega} \in \mathbb{R}^{I_2 \times (R+P)}$ be a given matrix and a Gaussian random matrix respectively with $P \geq 2$

Algorithm 3: Classical randomized subspace method for computation of the Truncated SVD [32]

Input : A tensor $\mathbf{X} \in \mathbb{R}^{I_1 \times I_2}$; a target tubal rank R ; Oversampling P and the power iteration q .

Output: Truncated t-SVD: $\mathbf{X} \cong \mathbf{U}\mathbf{S}\mathbf{V}^T$

- 1 $\mathbf{\Omega} = \text{randn}(I_2, P + R)$;
- 2 $[\mathbf{Q}^{(1)}, \sim] = \text{qr}(\mathbf{X}\mathbf{\Omega})$;
- 3 **for** $i = 1, 2, \dots, q$ **do**
- 4 $[\mathbf{Q}^{(2)}, \sim] = \text{qr}(\mathbf{X}\mathbf{Q}^{(1)})$;
- 5 $[\mathbf{Q}^{(1)}, \sim] = \text{qr}(\mathbf{X}^T \mathbf{Q}^{(2)})$;
- 6 **end**
- 7 $[\mathbf{Q}^{(2)}, \mathbf{R}] = \text{qr}(\mathbf{X}^T \mathbf{Q}^{(1)})$;
- 8 $[\widehat{\mathbf{V}}, \mathbf{S}, \widehat{\mathbf{U}}] = \text{Truncated SVD}(\mathbf{R}, R)$;
- 9 $\mathbf{V} = \mathbf{Q}^{(1)} \widehat{\mathbf{V}}$;
- 10 $\mathbf{U} = \mathbf{Q}^{(2)} \widehat{\mathbf{U}}$

Algorithm 4: Randomized truncated SVD with an arbitrary number of passes [18]

Input : A tensor $\mathbf{X} \in \mathbb{R}^{I_1 \times I_2}$; a target tubal rank R ; Oversampling P and the budget of number of passes v .

Output: Truncated t-SVD: $\mathbf{X} \cong \mathbf{U}\mathbf{S}\mathbf{V}^T$

- 1 $\mathbf{Q}^{(1)} = \text{randn}(I_2, P + R)$;
- 2 **for** $i = 1, 2, \dots, v$ **do**
- 3 **if** i is odd **then**
- 4 $[\mathbf{Q}^{(2)}, \mathbf{R}^{(2)}] = \text{qr}(\mathbf{X}\mathbf{Q}^{(1)})$;
- 5 **else**
- 6 $[\mathbf{Q}^{(1)}, \mathbf{R}^{(1)}] = \text{qr}(\mathbf{X}^T \mathbf{Q}^{(2)})$;
- 7 **end**
- 8 **end**
- 9 **if** v is even **then**
- 10 $[\widehat{\mathbf{V}}, \underline{\mathbf{S}}, \widehat{\mathbf{U}}] = \text{Truncated SVD}(\mathbf{R}^{(1)}, R)$;
- 11 **else**
- 12 $[\widehat{\mathbf{U}}, \underline{\mathbf{S}}, \widehat{\mathbf{V}}] = \text{Truncated SVD}(\mathbf{R}^{(2)}, R)$;
- 13 **end**
- 14 $\mathbf{V} = \mathbf{Q}^{(1)} \widehat{\mathbf{V}}$;
- 15 $\mathbf{U} = \mathbf{Q}^{(2)} \widehat{\mathbf{U}}$;

Algorithm 5: Classical randomized subspace method for computation of the Truncated t-SVD [23]

Input : A tensor $\underline{\mathbf{X}} \in \mathbb{R}^{I_1 \times I_2 \times I_3}$; a target tubal rank R ; Oversampling P and the power iteration q .

Output: Truncated t-SVD: $\underline{\mathbf{X}} \cong \underline{\mathbf{U}} * \underline{\mathbf{S}} * \underline{\mathbf{V}}^T$

- 1 $\underline{\mathbf{\Omega}} = \text{randn}(I_2, P + R, I_3)$;
- 2 $[\underline{\mathbf{Q}}^{(1)}, \sim] = \text{qr}(\underline{\mathbf{X}} * \underline{\mathbf{\Omega}})$;
- 3 **for** $i = 1, 2, \dots, q$ **do**
- 4 $[\underline{\mathbf{Q}}^{(2)}, \sim] = \text{qr}(\underline{\mathbf{X}} * \underline{\mathbf{Q}}^{(1)})$;
- 5 $[\underline{\mathbf{Q}}^{(1)}, \sim] = \text{qr}(\underline{\mathbf{X}}^T * \underline{\mathbf{Q}}^{(2)})$;
- 6 **end**
- 7 $[\underline{\mathbf{Q}}^{(2)}, \underline{\mathbf{R}}] = \text{qr}(\underline{\mathbf{X}}^T * \underline{\mathbf{Q}}^{(1)})$;
- 8 $[\underline{\widehat{\mathbf{V}}}, \underline{\mathbf{S}}, \underline{\widehat{\mathbf{U}}}] = \text{Truncated t-SVD}(\underline{\mathbf{R}}, R)$;
- 9 $\underline{\mathbf{V}} = \underline{\mathbf{Q}}^{(1)} * \underline{\widehat{\mathbf{V}}}$;
- 10 $\underline{\mathbf{U}} = \underline{\mathbf{Q}}^{(2)} * \underline{\widehat{\mathbf{U}}}$

Algorithm 6: Proposed pass efficient randomized truncated t-SVD with an arbitrary number of passes

Input : A tensor $\underline{\mathbf{X}} \in \mathbb{R}^{I_1 \times I_2 \times I_3}$; a target tubral rank R ; Oversampling P and the budget of number of passes v .

Output: Truncated t-SVD: $\underline{\mathbf{X}} \cong \underline{\mathbf{U}} * \underline{\mathbf{S}} * \underline{\mathbf{V}}^T$

```

1  $\underline{\mathbf{Q}}^{(1)} = \text{randn}(I_2, P + R, I_3)$ ;
2 for  $i = 1, 2, \dots, v$  do
3   if  $i$  is odd then
4      $[\underline{\mathbf{Q}}^{(2)}, \underline{\mathbf{R}}^{(2)}] = \text{qr}(\underline{\mathbf{X}} * \underline{\mathbf{Q}}^{(1)})$ ;
5   else
6      $[\underline{\mathbf{Q}}^{(1)}, \underline{\mathbf{R}}^{(1)}] = \text{qr}(\underline{\mathbf{X}}^T * \underline{\mathbf{Q}}^{(2)})$ ;
7   end
8 end
9 if  $v$  is even then
10   $[\widehat{\mathbf{V}}, \widehat{\mathbf{S}}, \widehat{\mathbf{U}}] = \text{Truncate t-SVD}(\underline{\mathbf{R}}^{(1)}, R)$ ;
11 else
12   $[\widehat{\mathbf{U}}, \widehat{\mathbf{S}}, \widehat{\mathbf{V}}] = \text{Truncated t-SVD}(\underline{\mathbf{R}}^{(2)}, R)$ ;
13 end
14  $\underline{\mathbf{V}} = \underline{\mathbf{Q}}^{(1)} * \widehat{\mathbf{V}}$ ;
15  $\underline{\mathbf{U}} = \underline{\mathbf{Q}}^{(2)} * \widehat{\mathbf{U}}$ ;
```

being the oversampling parameter. Suppose $\underline{\mathbf{Q}}$ is obtained from Algorithm 3, then

$$\mathbb{E}(\|\underline{\mathbf{X}} - \underline{\mathbf{Q}}\underline{\mathbf{Q}}^T \underline{\mathbf{X}}\|_F^2) \leq \left(1 + \frac{R}{P-1} \tau_R^{4q}\right) \left(\sum_{j=R+1}^{\min\{I_1, I_2\}} \sigma_j^2\right)$$

where R is a target truncation term, q is the power iteration, σ_j is the j -th singular value of $\underline{\mathbf{X}}$, and $\tau_R = \sigma_{R+1}/\sigma_R \ll 1$ is the singular value gap.

It is not difficult to check that for an even number of passes, e.g. $v = 2q + 2$, Algorithm 4 is equivalent to Algorithm 3, so, Theorem 1 can be used for its error analysis. However, for an odd number of passes, the error analysis of Algorithm 4 is presented in Theorem 2. We will use this to derive the average Frobenius error for Algorithm 6. Please note that in [18], some average error bounds (in spectral norm) have been proven for Algorithm 4, but here we consider the Frobenius norm. This helps to obtain an average error bound of the approximations achieved by our proposed Algorithm 6.

Theorem 2. (Average Frobenius error for Algorithm 4). Let $\underline{\mathbf{X}} \in \mathbb{R}^{I_1 \times I_2}$ and $\underline{\mathbf{Q}}^{(1)} \in \mathbb{R}^{I_2 \times (R+P)}$ be a given matrix and a Gaussian random matrix respectively with $P \geq 2$ being the oversampling parameter. Suppose $\underline{\mathbf{Q}}$ is obtained from Algorithm 4, with an odd number of passes v , then

$$\mathbb{E}(\|\underline{\mathbf{X}} - \underline{\mathbf{X}}\underline{\mathbf{Q}}\underline{\mathbf{Q}}^T\|_F^2) \leq \left(1 + \frac{R}{P-1} \tau_R^{2(2v-1)}\right) \left(\sum_{j=R+1}^{\min\{I_1, I_2\}} \sigma_j^2\right)$$

where R is a target truncation term, q is the power iteration, σ_j is the j -th singular value of $\underline{\mathbf{X}}$, and $\tau_R = \sigma_{R+1}/\sigma_R \ll 1$ is the singular value gap.

Proof. See the Appendix. \square

Theorem 3 [23] provides the average error bound for Algorithm 5. Similar to the matrix case, Algorithm 6 is reduced to Algorithm 5 when an even number of passes is used and in turn Theorem 3 can be used for its error analysis. For the case of odd number of passes, we present Theorem 4 and its proof is quite similar to the proof of Theorem 3 [23].

Theorem 3. [23] Given an $I_1 \times I_2 \times I_3$ tensor $\underline{\mathbf{X}}$ and a Gaussian tensor $\underline{\Omega}$ of size $I_2 \times (R+P) \times I_3$, if $\underline{\mathbf{Q}}$ is obtained from Algorithm 5, then

$$\mathbb{E}(\|\underline{\mathbf{X}} - \underline{\mathbf{Q}} * \underline{\mathbf{Q}}^T * \underline{\mathbf{X}}\|_F) \leq \left(\frac{1}{I_3} \sum_{i=1}^{i=I_3} \left(1 + \frac{R}{P-1} (\tilde{\tau}_R^{(i)})^{4q}\right) \left(\sum_{j>R} (\tilde{\sigma}_j^{(i)})^2\right)\right)^{1/2}$$

where R is a target truncation term, $P \geq 2$ is the oversampling parameter, q is the power iteration, $\tilde{\sigma}_j^{(i)}$ is the i -th component of $\text{fft}(\underline{\mathbf{S}}(j, j, :), [], 3)$, and the singular value gap $\tilde{\tau}_R^{(i)} = \frac{\tilde{\sigma}_{R+1}^{(i)}}{\tilde{\sigma}_R^{(i)}} \ll 1$.

Theorem 4. Given an $I_1 \times I_2 \times I_3$ tensor $\underline{\mathbf{X}}$ and an $I_2 \times (R+P) \times I_3$ Gaussian tensor $\underline{\mathbf{Q}}^{(1)}$, if $\underline{\mathbf{Q}}$ is obtained from Algorithm 6, then

$$\mathbb{E}(\|\underline{\mathbf{X}} - \underline{\mathbf{Q}} * \underline{\mathbf{Q}}^T * \underline{\mathbf{X}}\|_F) \leq \left(\frac{1}{I_3} \sum_{i=1}^{i=I_3} \left(1 + \frac{R}{P-1} (\tilde{\tau}_R^{(i)})^{2(2v-1)}\right) \left(\sum_{j>R} (\tilde{\sigma}_j^{(i)})^2\right)\right)^{1/2}$$

where R is a target truncation term, $P \geq 2$ is the oversampling parameter, with an odd number of passes v , $\tilde{\sigma}_j^{(i)}$ is the i -th component of $\text{fft}(\underline{\mathbf{S}}(j, j, :), [], 3)$, and the singular value gap $\tilde{\tau}_R^{(i)} = \frac{\tilde{\sigma}_{R+1}^{(i)}}{\tilde{\sigma}_R^{(i)}} \ll 1$.

Proof. See the Appendix. \square

IV. APPLICATION TO TENSOR COMPLETION

The problem of recovering a data tensor from only a part of its components is known as *tensor completion* [13]. Let $\underline{\mathbf{X}} \in \mathbb{R}^{I_1 \times I_2 \times \dots \times I_N}$ be given with the corresponding observation index set $\underline{\Omega}$, which stores the location of the known (observed) elements. It is known that under the low-rank property assumption of the underlying original tensor, we can efficiently recover it from its incomplete form [13]. A widely used tensor decomposition formulation for the tensor completion problem is as follows [35], [13]

$$\begin{aligned} \min_{\underline{\mathbf{X}}} \quad & \|\mathbf{P}_{\underline{\Omega}}(\underline{\mathbf{X}}) - \mathbf{P}_{\underline{\Omega}}(\underline{\mathbf{M}})\|_F^2, \\ \text{s.t.} \quad & \text{Rank}(\underline{\mathbf{X}}) = R, \end{aligned} \quad (6)$$

where $\underline{\mathbf{M}}$ is the exact tensor. As described in [36], using an auxiliary variable $\underline{\mathbf{C}}$, the optimization problem (6) can be solved more conveniently by the following reformulation

$$\begin{aligned} \min_{\underline{\mathbf{X}}, \underline{\mathbf{C}}} \quad & \|\underline{\mathbf{X}} - \underline{\mathbf{C}}\|_F^2, \\ \text{s.t.} \quad & \text{Rank}(\underline{\mathbf{X}}) = R, \\ & \mathbf{P}_{\underline{\Omega}}(\underline{\mathbf{C}}) = \mathbf{P}_{\underline{\Omega}}(\underline{\mathbf{M}}) \end{aligned} \quad (7)$$

and we can alternatively solve optimization problem (6) over variables $\underline{\mathbf{X}}$ and $\underline{\mathbf{C}}$. Thus, the solution to the minimization problem (6) can be approximated by the following iterative procedure

$$\underline{\mathbf{X}}^{(n)} \leftarrow \mathcal{L}(\underline{\mathbf{C}}^{(n)}), \quad (8)$$

$$\underline{\mathbf{C}}^{(n+1)} \leftarrow \underline{\Omega} \otimes \underline{\mathbf{M}} + (\underline{\mathbf{1}} - \underline{\Omega}) \otimes \underline{\mathbf{X}}^{(n)}, \quad (9)$$

where \mathcal{L} is an operator to compute a low-rank tensor approximation of the data tensor $\underline{\mathbf{X}}^{(n)}$ and $\underline{\mathbf{1}}$ is a tensor whose all components are equal to one. Note that Equation (8) solves the minimization problem (7) over $\underline{\mathbf{X}}$ for fixed variable $\underline{\mathbf{C}}$. Also Equation (9) solves the minimization problem (7) over $\underline{\mathbf{C}}$ for fixed variable $\underline{\mathbf{X}}$. The algorithm consists of two main steps, *low-rank tensor approximation* (8) and *Masking computation* (9). It starts from the initial incomplete data tensor $\underline{\mathbf{X}}^{(0)}$ with the corresponding observation index set $\underline{\Omega}$ and sequentially improves the approximate solution till some stopping criterion is satisfied or the maximum number of iterations is reached. We do not need to compute the term $\underline{\Omega} \otimes \underline{\mathbf{M}}$ at each iteration because it is just the initial data tensor $\underline{\mathbf{X}}^{(0)}$. The filtering/smoothing procedure is a known technique in signal processing community to improve the image quality. Indeed, in the above procedure, we exploit this idea and smooths out the tensor $\underline{\mathbf{C}}^{(n+1)}$ before applying the low tensor rank approximation operator \mathcal{L} to get better results. In the simulation section, we show the difference of between the results achieved by using the smoothing strategy with the one without this procedure. The first step is computationally expensive steps especially when a large number of iterations is required for convergence or the data tensor is quite large. Here, we use our randomized pass-efficient Algorithm 6 instead of the deterministic counterparts. The experimental results show that this algorithm provides promising results with low computational cost.

V. SIMULATIONS

In this section, we test the proposed randomized algorithm on synthetic and real-world datasets. All numerical simulations were performed on a laptop computer with 2.60 GHz Intel(R) Core(TM) i7-5600U processor and 8GB memory. The Peak Signal-to-Noise Ratio (PSNR) and relative error have been utilized to evaluate the performance of the proposed algorithm. The PSNR of two images $\underline{\mathbf{X}}$ and $\underline{\mathbf{Y}}$ is defined as

$$\text{PSNR} = 10 \log 10 \left(\frac{\|\underline{\mathbf{X}}\|_{\infty}}{\|\underline{\mathbf{X}} - \underline{\mathbf{Y}}\|_F} \right).$$

The relative error is also defined as

$$e(\hat{\underline{\mathbf{X}}}) = \frac{\|\underline{\mathbf{X}} - \hat{\underline{\mathbf{X}}}\|_F}{\|\underline{\mathbf{X}}\|_F},$$

where $\underline{\mathbf{X}}$ is the original tensor and $\hat{\underline{\mathbf{X}}}$ is the approximated tensor.

Example 1. In this experiment, we generate a tensor $\underline{\mathbf{X}} \in \mathbb{R}^{500 \times 500 \times 500}$ with tubal rank 15. We set the oversampling parameter $P = 5$ and applied Algorithm 6 with tubal rank $R = 10$ with different number of passes over the data tensor $\underline{\mathbf{X}}$. In

Figure 2 (right), we report the relative error versus the number of passes. The results show that with $v = 2, 3$ passes, we can achieve quite good results and for larger number of passes the accuracy is increased while the computational complexity is also higher. In Figure 2 (left), we report the running time of Algorithm 6 for different numbers of passes. Please note that the benefit of Algorithm 6 compared with Algorithm 3 is that it does not need to necessarily pass the original data tensor $\underline{\mathbf{X}}$ four times and with only 2 passes, we can achieve reasonable results. Since the synthetic data tensor used in this example was noiseless, the performance of Algorithm 6 for two and three passes was negligible. In Examples 2 and 3, we illustrate that for the real-world datasets (images and videos), the results of two and three passes are significant.

Example 2. In this example, we apply the proposed algorithm to compress color images. To this end, we consider the “Kodim03” and “Kodim23” color images included in the Kodak dataset¹. We set overparameter $P = 6$ and apply Algorithm 6 with tubal rank $R = 40$ and for different number of passes. The reconstructed images and corresponding results including relative error, PSNR and running time achieved by the proposed algorithm are reported in Figure 3. As can be seen, the higher the number of passes, the better performance of the images and the higher computational cost.

Example 3. In this experiment we examine Algorithm 6 for compressing the video datasets. We have used the “Foreman” and “News” videos from [37]. Both videos are 3rd order tensors and of size $144 \times 176 \times 300$. We set oversampling parameter $P = 5$ and apply the proposed algorithm for computing t-SVD with the tubal rank $R = 20$. For this tubal rank, we achieve the compression ratio 3.7271. The PSNR of some random samples of the frames for the mentioned two videos and different number of passes are reported in Figure 4. Beside, the PSNR of all frames of both videos are shown in Figure 5 (upper). The corresponding running times can be seen in Figure 5 (bottom). Here, again the same results as the previous two simulations are achieved and using more passes over the video dataset, we achieve better results with the higher computational cost.

Example 4. In this simulation, we examine the efficiency of Algorithm 6 for the tensor completion task described in Section IV. Here, we use both images and videos in our experiments. First, we consider four color images taken from Kodak dataset (“Kodim03”, “Kodim15”, “Kodim16”, “Kodim23”). The size of these images are $512 \times 768 \times 3$ and we remove 80% of the pixels randomly. Then apply the completion procedure described in Section IV with the tubal rank $R = 30$ and using Algorithm 6 with two passes ($v = 2$) and oversampling parameter $P = 10$. The reconstructed images are displayed in Figure 6. The results show the good performance of the proposed algorithm for the image completion task. We next considered three videos “Akiyo”, “Foreman”, and “News”[37] which are 3rd order tensors of

¹<http://www.cs.albany.edu/~xypan/research/snr/Kodak.html>

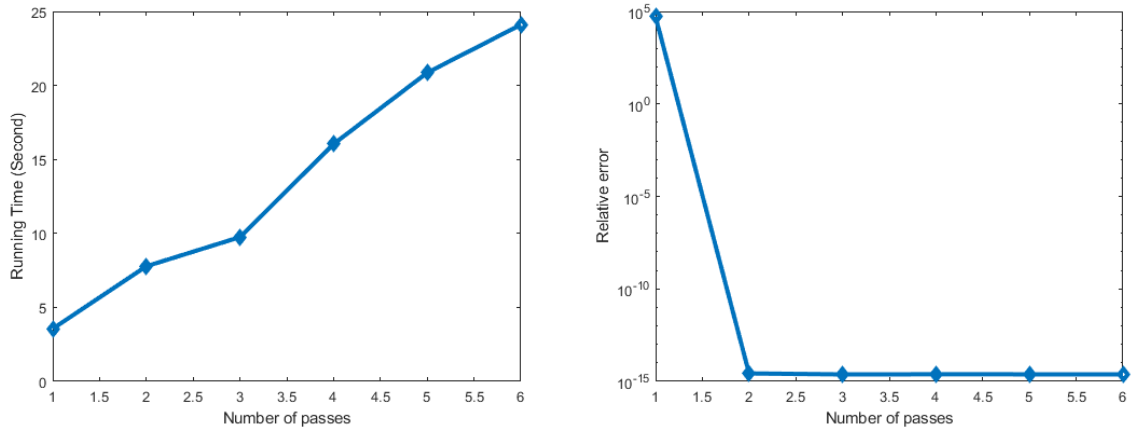


Fig. 2. Example 1. Running time and relative error of the proposed algorithm for a synthetic data tensor of size $500 \times 500 \times 500$ and tubal rank $R = 15$ using different number of passes.

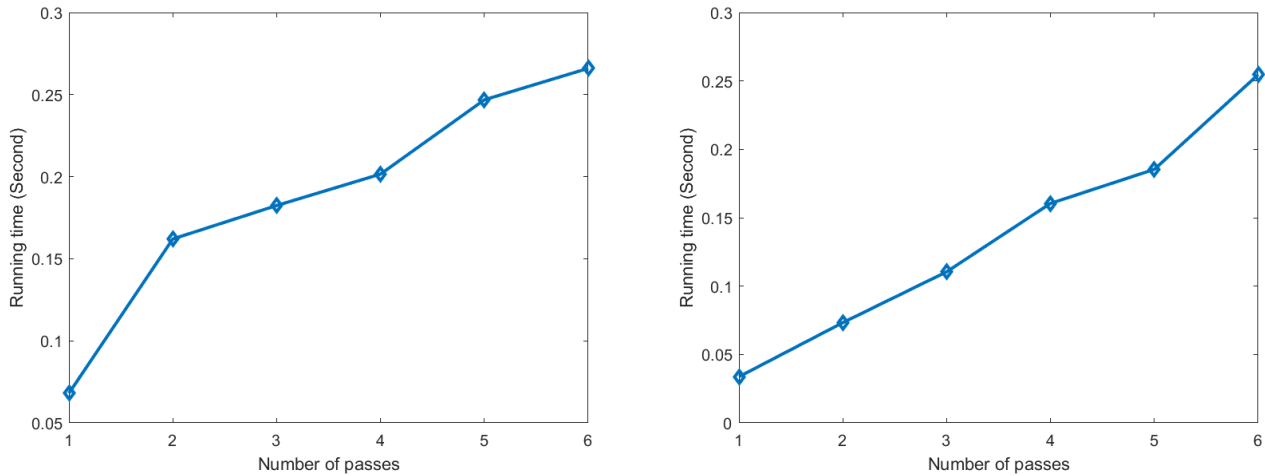
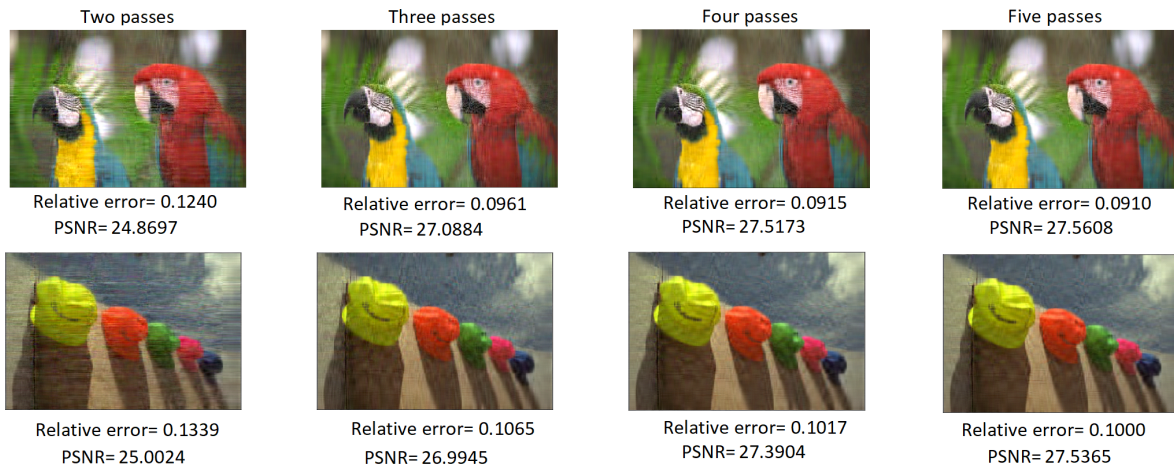


Fig. 3. Example 2. (Upper) The reconstruction of the “Kodim23” and the “Kodim03” images using the proposed algorithm for the tubal rank $R = 20$ and different number of passes (Bottom) The running time of the proposed algorithm for computation of the truncated t-SVD for the “Kodim23” image (left) and the “Kodim03” image (right) with the tubal rank $R = 40$ and using different number of passes.

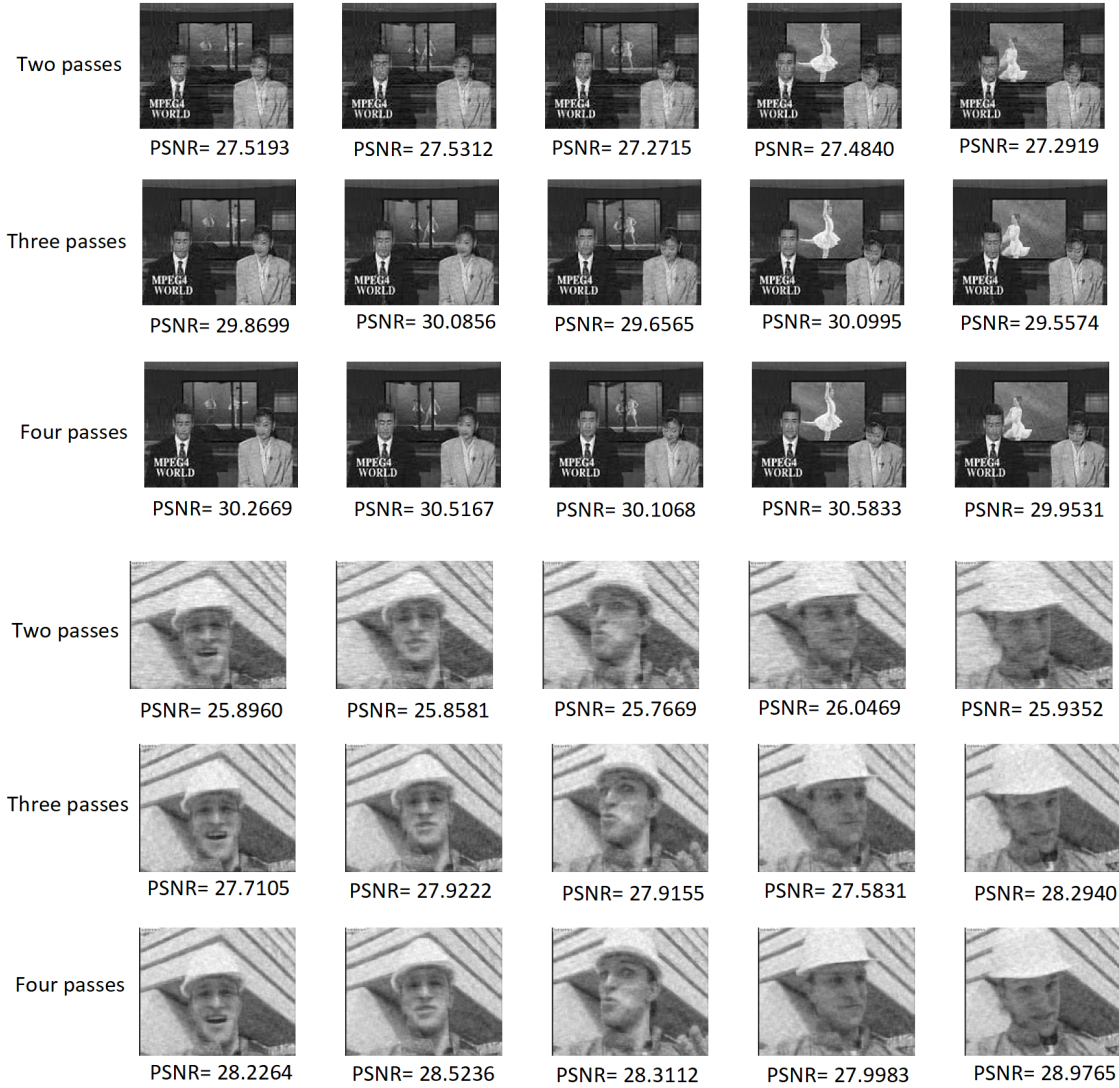


Fig. 4. Example 3. Reconstruction of some random samples of frames of the “News” and the “Foreman” videos using the proposed algorithm with the tubal rank $R = 20$ and different number of passes.

size $176 \times 144 \times 300$ (collocation of 300 frames or black and white images). We remove 70% of the pixels of the mentioned videos randomly. With the same procedure described for the images, we used our proposed pass-efficient algorithm with two passes ($v = 2$), the oversampling parameter $P = 10$, and the tubal rank $R = 15$ to reconstruct the incomplete videos. The PSNR of all reconstructed frames of the “Akiyo” video are shown in Figure 6 (upper). Also, the original, the observed and the reconstruction of some frames are displayed in Figure 7 (bottom). The obtained results for the “News” and the “Foreman” videos are reported in Figures 8 and 9, respectively. The results clearly indicate the efficiency of the proposed algorithm.

VI. CONCLUSION AND FUTURE WORKS

In this paper, a pass-efficient randomized algorithms was proposed for computation of the tensor SVD (t-SVD). In contrary to the classical randomized subspace algorithms which

needs an even number of passes over the data tensor, it can find a low tubal rank approximation of a 3rd order tensor for an arbitrary number of passes. We apply the proposed algorithm for reconstructing images with missing pixels. The extensive simulation results verifies the correctness and efficiency of the proposed algorithm. In our future work, we extend the block Krylov subspace algorithms to the tensor case based on the t-product and also proposing efficient single-pass algorithms for computation of the t-SVD.

VII. APPENDIX

This proof of Theorem 2 is almost the same as the proof of Theorem 1 presented in [23]. In fact they worked on the matrix $(\mathbf{X}\mathbf{X}^T)^v \mathbf{X}$ and here we consider $\mathbf{Y} = (\mathbf{X}^T \mathbf{X})^v$. However, due to some tricky modifications, we provide the details.

Let $\mathbf{X} = [\mathbf{U}_1, \mathbf{U}_2] \begin{bmatrix} \Sigma_1 & \mathbf{0} \\ \mathbf{0} & \Sigma_2 \end{bmatrix} \begin{bmatrix} \mathbf{V}_1^T \\ \mathbf{V}_2^T \end{bmatrix}$ and define $\Omega_1 = \mathbf{V}_1^T \Omega$, $\Omega_2 = \mathbf{V}_2^T \Omega$ where Σ_1 and Σ_2 are square. Now, from

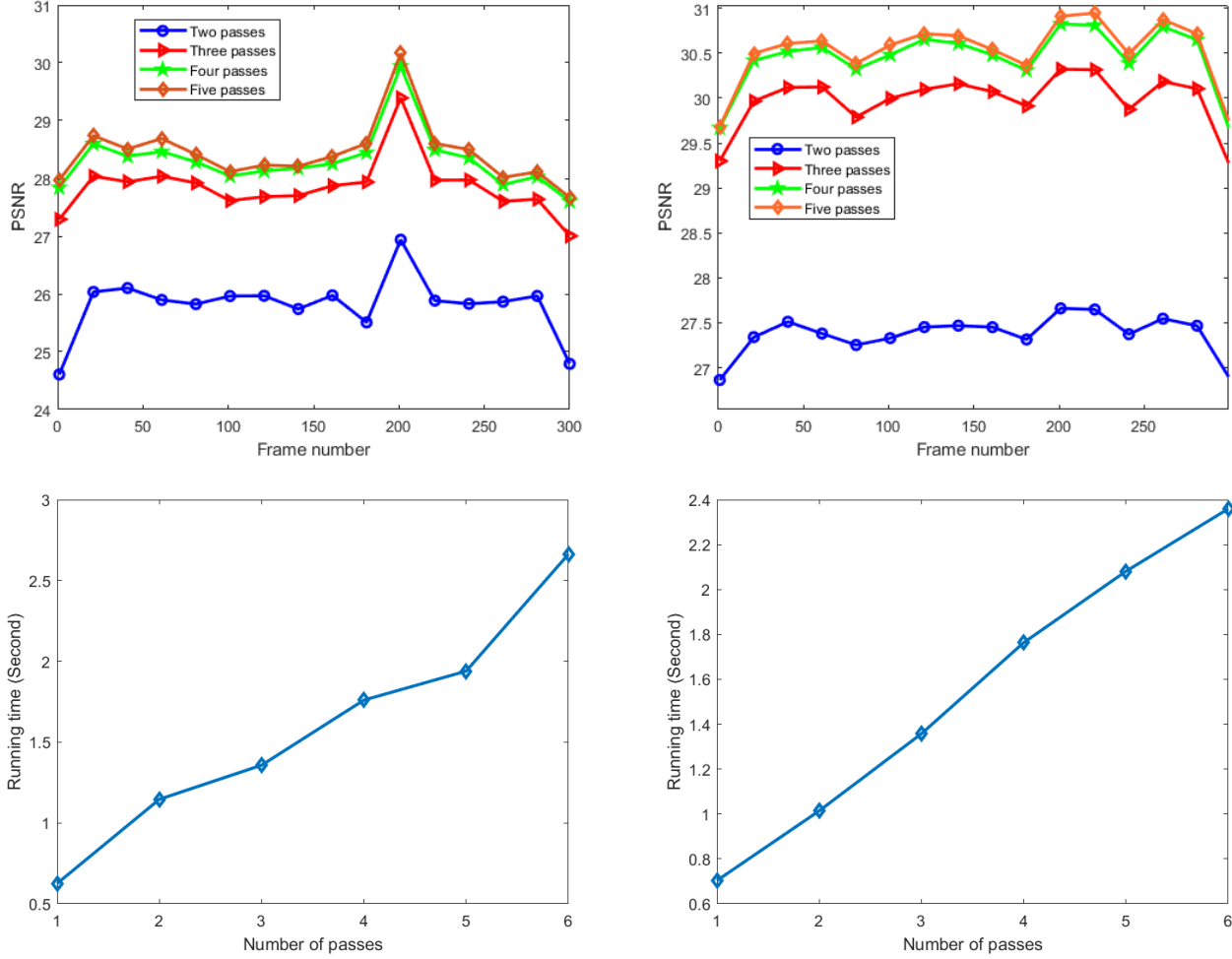


Fig. 5. Example 3. (Upper) The performance of the proposed algorithm for the video compression for different number of passes and the tubal rank $R = 20$ (left for the “Foreman” video and right is for the “News” video). (Bottom). The running time of the proposed algorithm for different number of passes and the tubal rank $R = 20$ (left for the “Foreman” video and right is for the “News” video)

straightforward computations we have

$$\mathbf{Y} = (\mathbf{X}^T \mathbf{X})^v \boldsymbol{\Omega} = \begin{bmatrix} \mathbf{V}_1 & \mathbf{V}_2 \end{bmatrix} \begin{bmatrix} \boldsymbol{\Sigma}_1^{2v} & \mathbf{0} \\ \mathbf{0} & \boldsymbol{\Sigma}_2^{2v} \end{bmatrix} \begin{bmatrix} \mathbf{V}_1^T \\ \mathbf{V}_2^T \end{bmatrix} \boldsymbol{\Omega} = \begin{bmatrix} \mathbf{V}_1 & \mathbf{V}_2 \end{bmatrix} \begin{bmatrix} \boldsymbol{\Sigma}_1^{2v} & \mathbf{0} \\ \mathbf{0} & \boldsymbol{\Sigma}_2^{2v} \end{bmatrix} \begin{bmatrix} \boldsymbol{\Omega}_1 \\ \boldsymbol{\Omega}_2 \end{bmatrix},$$

and consider the orthogonal projector $\mathbf{P}_V = \mathbf{V}\mathbf{V}^T$. To prove Theorem 2, we need to first prove the following theorem.

Theorem 5. Let $\mathbf{X} \in \mathbb{R}^{I \times J}$ with the SVD $\mathbf{X} = \mathbf{U}\boldsymbol{\Sigma}\mathbf{V}^T$ and $k \geq 0$ be a fixed parameter. Choose $\boldsymbol{\Omega}_1$ and $\boldsymbol{\Omega}_2$ as above and assume that $\boldsymbol{\Omega}_1$ is of full rank. Compute the \mathbf{Q} using Algorithm 4 for an odd number of passes v , then the approximation error satisfies

$$\|\mathbf{X}(\mathbf{I} - \mathbf{Q}\mathbf{Q}^T)\|_F^2 \leq \|\boldsymbol{\Sigma}_2\|_F^2 + \tau^{2(2v-1)} \|\boldsymbol{\Sigma}_2 \boldsymbol{\Omega}_2 \boldsymbol{\Omega}_1^\dagger\|_F^2. \quad (10)$$

Proof. Define matrices \mathbf{Z} and \mathbf{F} as

$$\mathbf{Z} = \mathbf{V}^T \mathbf{Y} \boldsymbol{\Omega}_1^\dagger \boldsymbol{\Sigma}_1^{-2v} = \begin{bmatrix} \mathbf{I} \\ \mathbf{F} \end{bmatrix}, \quad \mathbf{F} \equiv \boldsymbol{\Sigma}_2^{2v} \boldsymbol{\Omega}_2 \boldsymbol{\Omega}_1^\dagger \boldsymbol{\Sigma}_1^{-2v}. \quad (11)$$

From the construction of \mathbf{Z} , we have

$$\text{Range}(\mathbf{Z}) \subset \text{Range}(\mathbf{Y}) \subset \text{Range}(\mathbf{V}^T \mathbf{Y}) \subset \text{Range}(\mathbf{V}^T \mathbf{Q}). \quad (12)$$

It is not difficult to see

$$\|\mathbf{X}(\mathbf{I} - \mathbf{Q}\mathbf{Q}^T)\|_F^2 = \|\mathbf{U}\boldsymbol{\Sigma}\mathbf{V}^T(\mathbf{I} - \mathbf{P}_Q)\|_F^2 = \|\boldsymbol{\Sigma}\mathbf{V}^T(\mathbf{I} - \mathbf{P}_Q)\|_F^2, \quad (13)$$

and from (12)-13 together with [Propositions 8.4 and 8.5 in [14]], we have

$$\|\boldsymbol{\Sigma}\mathbf{V}^T(\mathbf{I} - \mathbf{P}_Q)\|_F^2 = \|\boldsymbol{\Sigma}\mathbf{V}^T(\mathbf{I} - \mathbf{P}_Q)\mathbf{V}\boldsymbol{\Sigma}^T\|_F \leq \|\boldsymbol{\Sigma}(\mathbf{I} - \mathbf{P}_{V^T Q})\boldsymbol{\Sigma}^T\|_F = \|(\mathbf{I} - \mathbf{P}_Z)\boldsymbol{\Sigma}^T\|_F^2. \quad (14)$$

Similar to [14], [23], we can prove

$$(\mathbf{I} - \mathbf{P}_Z)\boldsymbol{\Sigma}^T = \begin{bmatrix} (\mathbf{I} + \mathbf{F}^T \mathbf{F})^{-1} \mathbf{F}^T \mathbf{F} \boldsymbol{\Sigma}_1 \\ (\mathbf{I} - \mathbf{F}(\mathbf{I} + \mathbf{F}^T \mathbf{F})^{-1}) \mathbf{F}^T \boldsymbol{\Sigma}_2 \end{bmatrix},$$

and so we come at

$$\|(\mathbf{I} - \mathbf{P}_Z)\boldsymbol{\Sigma}^T\|_F^2 = \|(\mathbf{I} + \mathbf{F}^T \mathbf{F})^{-1} \mathbf{F}^T \mathbf{F} \boldsymbol{\Sigma}_1\|_F^2 + \|(\mathbf{I} - \mathbf{F}(\mathbf{I} + \mathbf{F}^T \mathbf{F})^{-1}) \mathbf{F}^T \boldsymbol{\Sigma}_2\|_F^2. \quad (15)$$



Fig. 6. Example 4. The comparison between the original, the observed (with 80% missing pixels) and the reconstructed images using the completion algorithm based on the proposed algorithm with two passes and the tubal rank 30.

Now, we bound two terms of (15). For the first term, consider

$$\begin{aligned} \|(\mathbf{I} + \mathbf{F}^T \mathbf{F})^{-1} \mathbf{F}^T \mathbf{F} \Sigma_1\|_F^2 &\leq \|(\mathbf{I} + \mathbf{F}^T \mathbf{F})^{-1}\|_2 \|\mathbf{F} \Sigma_1\|_F \\ &\leq \|\mathbf{F} \Sigma_1\|_F, \end{aligned} \quad (16)$$

and for the second term, we get

$$\|(\mathbf{I} - \mathbf{F}(\mathbf{I} + \mathbf{F}^T \mathbf{F})^{-1}) \mathbf{F}^T \Sigma_2\|_F^2 \leq \|\Sigma_2\|_F^2, \quad (17)$$

because $\mathbf{I} - \mathbf{F}(\mathbf{I} + \mathbf{F}^T \mathbf{F})^{-1}) \mathbf{F}^T \preceq \mathbf{I}$, see [14]. From (13), (15), (16) and (17), we have

$$\|\mathbf{X}(\mathbf{I} - \mathbf{P}_Q)\|_F^2 \leq \|\mathbf{X}(\mathbf{I} - \mathbf{P}_Z)\|_F^2 \leq \|\Sigma_2\|_F^2 + \|\mathbf{F} \Sigma_1\|_F^2. \quad (18)$$

It is seen that $\mathbf{F} \Sigma_1 = \Sigma_2^{2v-1} (\Sigma_2 \Omega_2 \Omega_1^\dagger) \Sigma_1^{-2v+1}$ and with some straightforward computations we get

$$\begin{aligned} \|\mathbf{F} \Sigma_1\|_F &\leq \|\Sigma_2^{2v-1}\|_2 \|\Sigma_1^{-2v+1}\|_2 \|\Sigma_2 \Omega_2 \Omega_1^\dagger\|_F \\ &\leq \tau^{(2v-1)} \|\Sigma_2 \Omega_2 \Omega_1^\dagger\|_F. \end{aligned} \quad (19)$$

From (17) and (19), we can conclude the identity (10). \square

Proof of Theorem 2. Combining Theorem 5 and Theorem 10.5 in [14], the desired result can be achieved.

Proof of Theorem 4. From linearity of the expectation operator and relation (2) we have

$$\begin{aligned} \mathbb{E} \|\underline{\mathbf{X}} - \underline{\mathbf{X}} * \underline{\mathbf{Q}} * \underline{\mathbf{Q}}^T\|_F^2 &\leq \\ \frac{1}{I_3} \left(\sum_{i=1}^{I_3} \mathbb{E} \|\widehat{\mathbf{X}}^{(i)} - \widehat{\mathbf{X}}^{(i)} \widehat{\mathbf{Q}}^{(i)} \widehat{\mathbf{Q}}^{(i)T}\|_F^2 \right), \end{aligned} \quad (20)$$

where $\widehat{\mathbf{X}}^{(i)} = \widehat{\mathbf{X}}(:, :, i)$ and $\widehat{\mathbf{Q}}^{(i)} = \widehat{\mathbf{Q}}(:, :, i)$. We can now use Theorem 2 to bound each term of summation (20) as follows

$$\begin{aligned} \mathbb{E} \|\widehat{\mathbf{X}}^{(i)} - \widehat{\mathbf{X}}^{(i)} \widehat{\mathbf{Q}}^{(i)} \widehat{\mathbf{Q}}^{(i)T}\|_F^2 &\leq \\ \frac{1}{I_3} \left(1 + \frac{R}{P-1} (\tau_R^{(i)})^{2(2q-1)} \right) &\left(\sum_{j>R} (\widehat{\sigma}_j^{(i)})^2 \right), \end{aligned}$$

and so we have

$$\begin{aligned} \mathbb{E} \|\underline{\mathbf{X}} - \underline{\mathbf{X}} * \underline{\mathbf{Q}} * \underline{\mathbf{Q}}^T\|_F^2 &\leq \\ \sum_{i_3=1}^{I_3} \frac{1}{I_3} \left(1 + \frac{R}{P-1} (\tau_R^{(i)})^{2(2q-1)} \right) &\left(\sum_{j>R} (\widehat{\sigma}_j^{(i)})^2 \right). \end{aligned}$$

It suffices to use the Hokder's identity

$$\mathbb{E} \|\underline{\mathbf{X}} - \underline{\mathbf{X}} * \underline{\mathbf{Q}} * \underline{\mathbf{Q}}^T\|_F \leq \left(\mathbb{E} \|\underline{\mathbf{X}} - \underline{\mathbf{X}} * \underline{\mathbf{Q}} * \underline{\mathbf{Q}}^T\|_F^2 \right)^{1/2}$$

to can get the desired result.

VIII. ACKNOWLEDGEMENT

The author was partially supported by the Ministry of Education and Science of the Russian Federation (grant 075.10.2021.068).

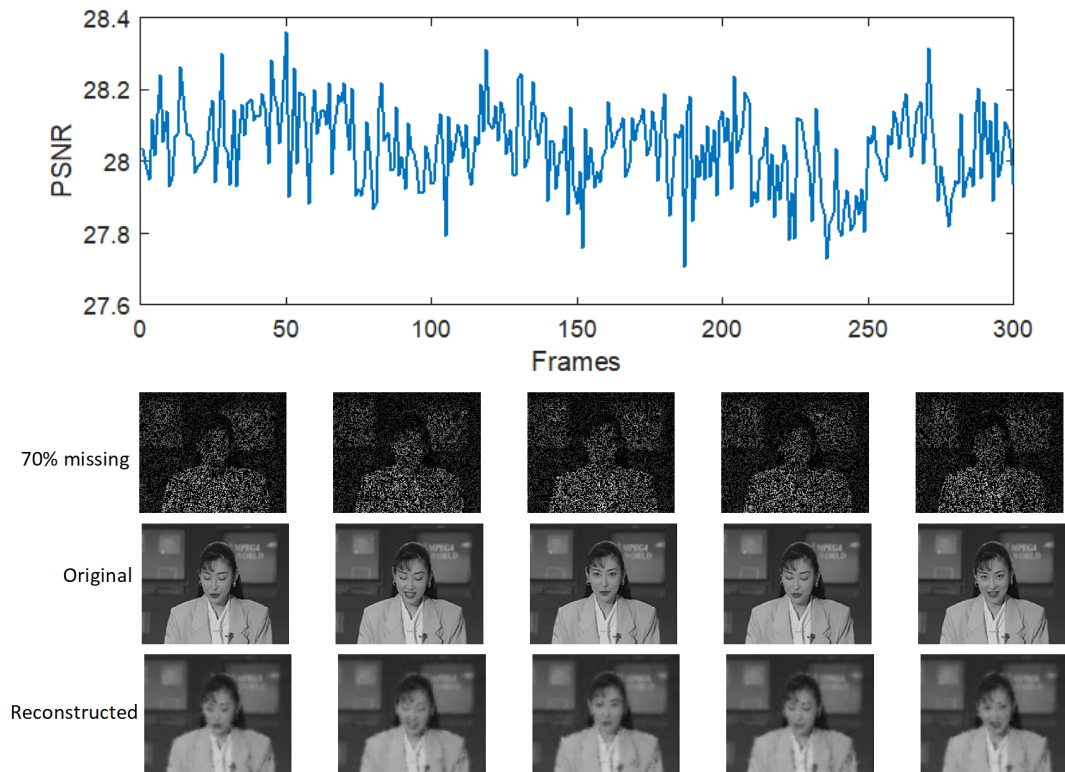


Fig. 7. Example 4. (Upper) The PSNR of all reconstructed frames of the “Akiyo” video using the completion procedure based on the proposed algorithm for the tubal rank $R = 15$ and two passes (Bottom) Visualization of some random samples of the original, the observed (70% missing pixels) and the reconstructed frames.

IX. DECLARATION

Conflicts of interests. The author declares that he has no conflict of interest with anything.

Ethical Approval. Ethical approval is not applicable for this article.

REFERENCES

- [1] F. L. Hitchcock, The expression of a tensor or a polyadic as a sum of products, *Journal of Mathematics and Physics* 6 (1-4) (1927) 164–189.
- [2] L. R. Tucker, Implications of factor analysis of three-way matrices for measurement of change, *Problems in measuring change* 15 (1963) 122–137.
- [3] L. R. Tucker, et al., The extension of factor analysis to three-dimensional matrices, *Contributions to mathematical psychology* 110119 (1964).
- [4] I. V. Oseledets, Tensor-train decomposition, *SIAM Journal on Scientific Computing* 33 (5) (2011) 2295–2317.
- [5] S. Östlund, S. Rommer, Thermodynamic limit of density matrix renormalization, *Physical review letters* 75 (19) (1995) 3537.
- [6] M. Espig, K. K. Naraparaju, J. Schneider, A note on tensor chain approximation, *Computing and Visualization in Science* 15 (6) (2012) 331–344.
- [7] Q. Zhao, G. Zhou, S. Xie, L. Zhang, A. Cichocki, Tensor ring decomposition, *arXiv preprint arXiv:1606.05535* (2016).
- [8] M. E. Kilmer, C. D. Martin, Factorization strategies for third-order tensors, *Linear Algebra and its Applications* 435 (3) (2011) 641–658.
- [9] M. E. Kilmer, K. Braman, N. Hao, R. C. Hoover, Third-order tensors as operators on matrices: A theoretical and computational framework with applications in imaging, *SIAM Journal on Matrix Analysis and Applications* 34 (1) (2013) 148–172.
- [10] W. Hackbusch, S. Kühn, A new scheme for the tensor representation, *Journal of Fourier analysis and applications* 15 (5) (2009) 706–722.
- [11] T. G. Kolda, B. W. Bader, Tensor decompositions and applications, *SIAM review* 51 (3) (2009) 455–500.
- [12] A. Cichocki, A.-H. Phan, Q. Zhao, N. Lee, I. Oseledets, M. Sugiyama, D. P. Mandic, et al., Tensor networks for dimensionality reduction and large-scale optimization: Part 2 applications and future perspectives, *Foundations and Trends® in Machine Learning* 9 (6) (2017) 431–673.
- [13] Q. Song, H. Ge, J. Caverlee, X. Hu, Tensor completion algorithms in big data analytics, *ACM Transactions on Knowledge Discovery from Data (TKDD)* 13 (1) (2019) 1–48.
- [14] N. Halko, P.-G. Martinsson, J. A. Tropp, Finding structure with randomness: Probabilistic algorithms for constructing approximate matrix decompositions, *SIAM review* 53 (2) (2011) 217–288.
- [15] O. A. Malik, S. Becker, Low-rank Tucker decomposition of large tensors using tensorsketch, in: *Advances in Neural Information Processing Systems*, 2018, pp. 10117–10127.
- [16] M. Che, Y. Wei, Randomized algorithms for the approximations of Tucker and the tensor train decompositions, *Advances in Computational Mathematics* (2018) 1–34.
- [17] O. A. Malik, S. Becker, A sampling-based method for tensor ring decomposition, in: *International Conference on Machine Learning, PMLR*, 2021, pp. 7400–7411.
- [18] E. K. Bjarkason, Pass-efficient randomized algorithms for low-rank matrix approximation using any number of views, *SIAM Journal on Scientific Computing* 41 (4) (2019) A2355–A2383.
- [19] C. Lu, J. Feng, Y. Chen, W. Liu, Z. Lin, S. Yan, Tensor robust principal component analysis with a new tensor nuclear norm, *IEEE transactions on pattern analysis and machine intelligence* 42 (4) (2019) 925–938.
- [20] E. Kernfeld, M. Kilmer, S. Aeron, Tensor–tensor products with invertible linear transforms, *Linear Algebra and its Applications* 485 (2015) 545–570.
- [21] G. Song, M. K. Ng, X. Zhang, Robust tensor completion using transformed tensor singular value decomposition, *Numerical Linear Algebra with Applications* 27 (3) (2020) e2299.
- [22] T.-X. Jiang, M. K. Ng, X.-L. Zhao, T.-Z. Huang, Framelet representation of tensor nuclear norm for third-order tensor completion, *IEEE Transactions on Image Processing* 29 (2020) 7233–7244.

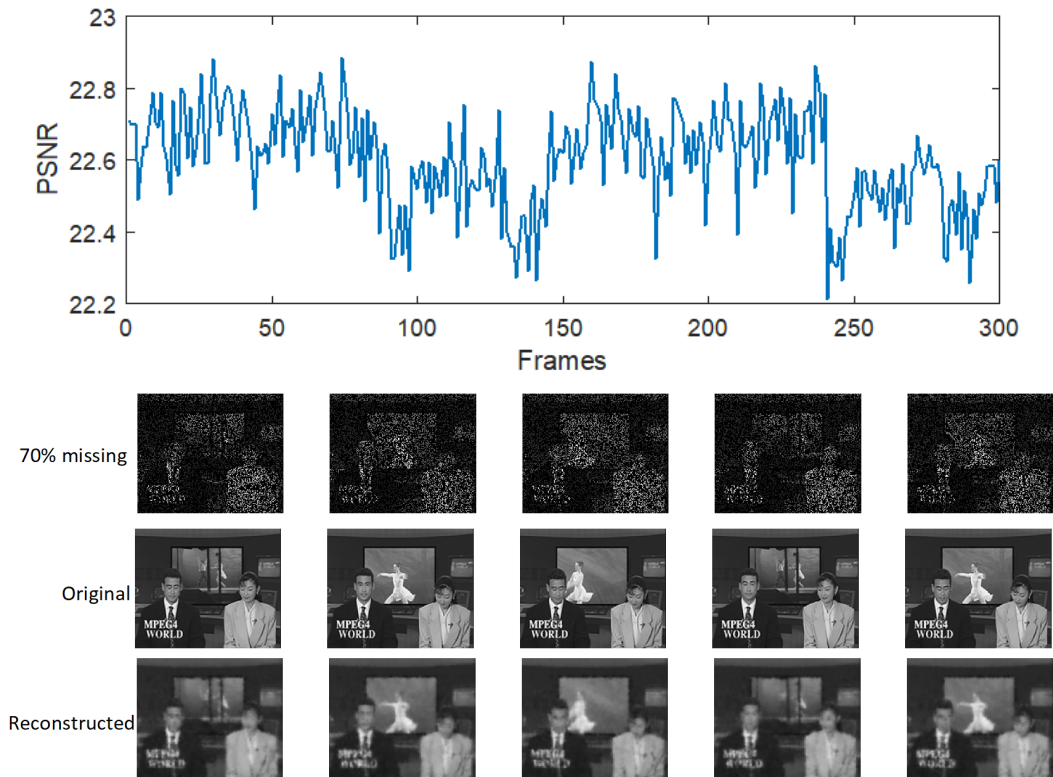


Fig. 8. Example 4. (Upper) The PSNR of all reconstructed frames of the “News” video using the completion procedure based on the proposed algorithm for the tubal rank $R = 15$ and two passes (Bottom) Visualization of some random samples of the original, the observed (70% missing pixels) and the reconstructed frames.

- [23] J. Zhang, A. K. Saibaba, M. E. Kilmer, S. Aeron, A randomized tensor singular value decomposition based on the t-product, *Numerical Linear Algebra with Applications* 25 (5) (2018) e2179.
- [24] K. Braman, Third-order tensors as linear operators on a space of matrices, *Linear Algebra and its Applications* 433 (7) (2010) 1241–1253.
- [25] D. F. Gleich, C. Greif, J. M. Varah, The power and arnoldi methods in an algebra of circulants, *Numerical Linear Algebra with Applications* 20 (5) (2013) 809–831.
- [26] C. D. Martin, R. Shafer, B. LaRue, An order-p tensor factorization with applications in imaging, *SIAM Journal on Scientific Computing* 35 (1) (2013) A474–A490.
- [27] S. Ahmadi-Asl, C. F. Caiafa, A. Cichocki, A. H. Phan, T. Tanaka, I. Osleledets, J. Wang, Cross tensor approximation methods for compression and dimensionality reduction, *IEEE Access* 9 (2021) 150809–150838.
- [28] L. Qi, G. Yu, T-singular values and t-sketching for third order tensors, *arXiv preprint arXiv:2103.00976* (2021).
- [29] M. Ding, P. Xie, A randomized singular value decomposition for third-order oriented tensors, *arXiv preprint arXiv:2203.02761* (2022).
- [30] H. Li, G. C. Linderman, A. Szlam, K. P. Stanton, Y. Kluger, M. Tygert, Algorithm 971: An implementation of a randomized algorithm for principal component analysis, *ACM Transactions on Mathematical Software (TOMS)* 43 (3) (2017) 28.
- [31] N. B. Erichson, S. Voronin, S. L. Brunton, J. N. Kutz, Randomized matrix decompositions using r, *arXiv preprint arXiv:1608.02148* (2016).
- [32] S. Voronin, P.-G. Martinsson, Rsvdpack: Subroutines for computing partial singular value decompositions via randomized sampling on single core, multi core, and gpu architectures, *arXiv preprint arXiv:1502.05366* 2 (2015) 16.
- [33] C. Battaglino, G. Ballard, T. G. Kolda, A practical randomized CP tensor decomposition, *SIAM Journal on Matrix Analysis and Applications* 39 (2) (2018) 876–901.
- [34] Y. Sun, Y. Guo, C. Luo, J. Tropp, M. Udell, Low-rank tucker approximation of a tensor from streaming data, *SIAM Journal on Mathematics of Data Science* 2 (4) (2020) 1123–1150.
- [35] E. J. Candès, B. Recht, Exact matrix completion via convex optimization, *Foundations of Computational mathematics* 9 (6) (2009) 717–772.
- [36] S. Ahmadi-Asl, M. G. Asante-Mensah, A. Cichocki, A.-H. Phan, I. Osleledets, J. Wang, Cross tensor approximation for image and video completion, *arXiv preprint arXiv:2207.06072* (2022).
- [37] <http://trace.eas.asu.edu/yuv/>.

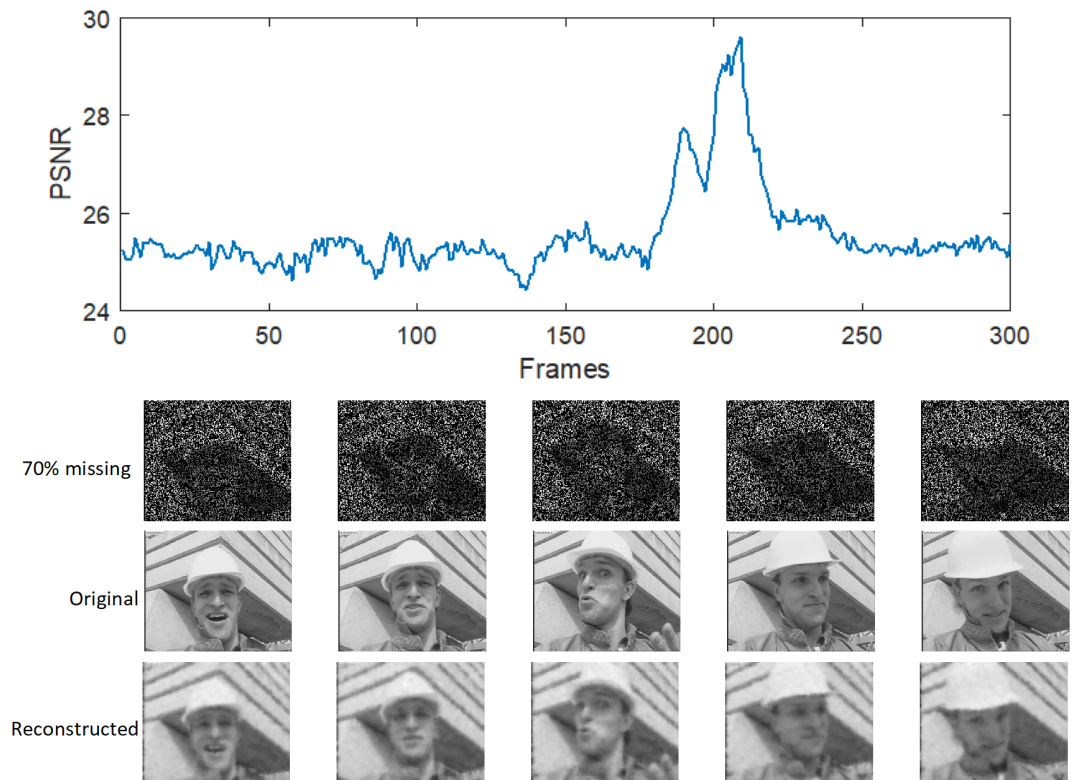


Fig. 9. Example 4. (Upper) The PSNR of all reconstructed frames of the “Foreman” video using the completion procedure based on the proposed algorithm for the tubal rank $R = 15$ and two passes (Bottom) Visualization of some random samples of the original, the observed (70% missing pixels) and the reconstructed frames.